# EVALUATING HEIGHT DIFFERENCES BETWEEN GLOBAL DIGITAL SURFACE MODELS AND ICESAT HEIGHTS AT FOOTPRINT GEOLOCATION

Fabian, ENßLE[1], Johannes, HEINZEL[2], Barbara, KOCH[3]

Department of Remote Sensing and Landscape Information Systems, Faculty of Forest and Environmental Sciences, University of Freiburg, Tennenbacherstraße 4, 79106 Freiburg i.Br., Germany

*fabian.enssle@felis.uni-freiburg.de[1] , johannes.heinzel@felis.uni-freiburg.de[2], ferninfo@felis.uni-freiburg.de[3]*

**Abstract**

Three Digital Elevation Models (DEMs) derived from satellite data have been evaluated. These are the SRTM90 and SRTM25 derived from the Shuttle Radar Topography Mission (SRTM) and the Global Digital Elevation Model Version 2 (GDEMV2) computed with data of the Advanced Spaceborne Thermal Emission and Reflection Radiometer (ASTER). The elevations obtained by the Geoscience Laser Altimeter System (GLAS) on board the Ice, Cloud and land Elevation Satellite (ICESat) are used to evaluate the vertical accuracy of the aforementioned DEMs. Elevation values are extracted at GLAS footprint centre coordinates. The study area is defined by the external borders of the federal state of Baden-Wuerttemberg, located in south-western Germany. An overall amount of 14615 elevation samples have been analyzed, where altitude information could be derived from all datasets. In addition to the spatial condition of intersecting height information, the heights of GLAS data product (Product GLA14, Version 31) were filtered for unsuitable elevation values. For evaluating the influence of different land use types, the land use map provided by the Office for the Environment, Measurements and Nature Conservation of Baden-Württemberg (LUBW) was used. To estimate the effect on elevation differences by surface slope, the latter was derived from SRTM25 data. Including all 14615 geolocations, results indicate the SRTM90 to have the best correlation with the ICESat heights. Mean differences and standard deviations between ICESat heights and the other elevation sources are: SRTM90 0.4m/10.1, SRTM25 -0.9m/7.8, GDEMV2 0.8m/9.3. Concerning absolute height differences the computed mean values and standard deviations are: SRTM90 6.5m/7.8, SRTM25 5.2m/6.0 and GDEMV2 6.9m/6.3. The slightest increase in mean deviation with increasing terrain slope class was observed in the GDEMV2 dataset.

**Keywords: DEM, DSM, DTM, SRTM25, SRTM90, ASTER GDEM, ICESat, GLAS, elevation, land use**

## INTRODUCTION

Digital Surface Models (DEM) by remotely sensed data are often the solely height information for remote areas. Besides the commercial high quality DEMs, produced by land survey offices or private companies, the freely available DEMs are widely in use. They are utilized for topographic correction of satellite images, calculation of slope or aspect for environmental analyses or construction planning. Different kinds of DEM's by satellite remotely sensed data do exist. Small scale DEMs with a ground resolution of few km² down to high resolution DEMs of 25m² ground resolution. When asked about the most suitable DEM for a project, it is important to know the vertical accuracy. We will evaluate three common elevation sources that have been produced by satellite data. Two DEMs by the Shuttle Radar Topography Mission (SRTM) with a ground resolution of approximately 90m/25m and the ASTER Global Digital Elevation Model Version 2 (GDEMV2) will be evaluated. The Geoscience Laser Altimeter System (GLAS) on board the Ice, Cloud and land Elevation Satellite (ICESat) provides well-suited elevation measurements for evaluating these continental DEMs [1]. Instead of the contiguous DEMs, ICESat elevation information is provided more sparsely in a stripe scanning pattern, but of approved highly precise elevation measurements [1, 2, 3, 4, 5].

For different geographic regions and DEM sources a variety of accuracy assessments have been made. [1] validated elevations from the SRTM mission by ICESat elevations. They found a mean of -0.6m with a standard deviation of 3.46 for low relief and tree cover. Accuracy is deteriorated with increasing slope or increasing vegetation cover. For a study area in the Tibetan Plateau [6] identified a strong correlation of SRTM elevations with ICESat elevations. An assessment of ASTER GDEM using comparison with SRTM and ICESat data was conducted by [7] for central China. An investigation of ASTER GDEM versus SRTM was carried out by [8]. They also used ICESat data for absolute reference. The second release (version 2) of ASTER GDEM was also evaluated against ICESat elevation measurements by [9].

While height differences between single data have already been examined by other authors, until now they have not been evaluated for a complete large area. Besides this, we want to examine the influence of surface slope and the effect of different land use classes. Since the effect of slope on GLAS height measurements is well known [10], we want examine which of the tested DEMs is most sensitive for sloped terrain.

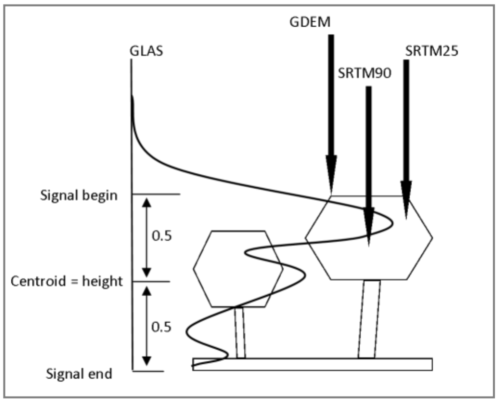


**Fig.1** Sketchy illustration of forest canopy penetration by GLAS (shown elevation determination is one of seven methods), GDEM, SRTM90 and SRTM25 due to different wavelengths used by remote sensors.

Because of the effects of different wavelengths on elevation computation and canopy penetration (Fig. 1), it is assumed that GLAS surface elevation, compared to the three other DEM heights, will be lower for forested and urban areas. The result of a subtraction of DEM values from ICESat heights should therefore be negative.

## STUDY AREA AND DATA

### Study Area

The extent of the study area for this investigation is the external boarder of the federal state Baden-Wuerttemberg of Germany (Fig. 2). The total land area of 35748km² is covered by mountain as well as by flat regions. The eastern part is built by the plain of the Upper Rhine valley. From this valley to the west the slopes of the Black Forest low mountain range arise. Further west the south-western German cuesta forms a series of plains separated by steep slopes.

### Data

The data collection for the SRTM was started in the year 2000 and comprised an eleven day mission [10]. The shuttle carried two different synthetic aperture radar systems. One of these radar systems operated within C-band and the other within X-band wavelengths (5.6cm and 3.1cm) [11]. The outcome of that mission is a worldwide topographic dataset with near-global coverage. The first release of the C-band derived elevation products was in the year 2003 with a degraded resolution of 3-arc seconds outside the US. The Consortium for Spatial Information (CGIAR-CSI) of the Consultative Group for International Agricultural Research (CGIAR) provides post processed DEM datasets of 3-arc seconds resolution (~ 90m). This product was used in Version 4 within this study. Data is delivered in geographic projection of WGS84 and vertical datum EGM96.

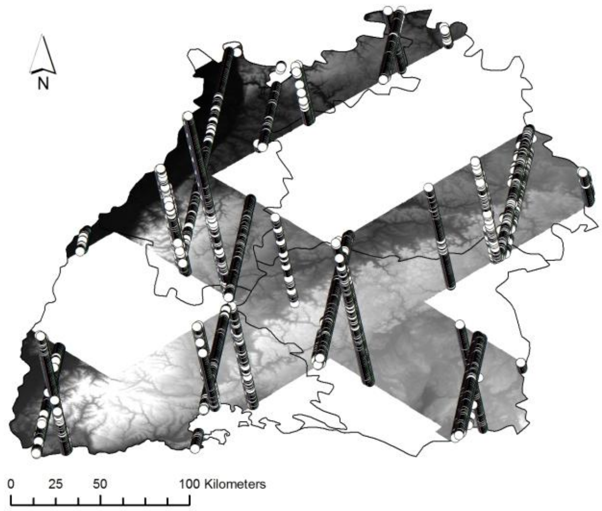


**Fig.2**: Extent of the federal state Baden-Württemberg with circular footprints of ICESat GLAS ground tracks (adjusted data) and available SRTM25 data.

The DEM derived from the X-band radar system is under charge of the German Aerospace Center (Deutsches Zentrum für Luft- und Raumfahrt, DLR) and the Italian Space Agency (ASI) [12]. This SRTM25 was made available for scientific purposes from end of May 2011 by DLR. This product was downloaded with a geographic projection of WGS84 and WGS84 ellipsoidal heights. It has a better ground resolution of approximately 25m x 25m compared to the SRTM90, but only exists in a global stripe pattern. Figure 2 illustrates the coverage by SRTM25 elevation data at the study area.

The ASTER GDEM data is property of the Japanese Ministry of Economy, Trade, and Industry (METI) and the United States National Aeronautics and Space Administration (NASA) [13]. Elevations are determined by an automated stereo-correlating algorithm. From 17th October 2011 on, the second version of ASTER GDEM is available. With a ground resolution of 30m x 30m, the data was obtained from Japan's Ground Data System. The GDEMV2 elevation product is delivered in the same projection and vertical datum as the SRTM90 (WGS84/EGM96).

The ICESat was lunched on 12$^{th}$ January 2003. The GLAS instrument on board ICESat had three lasers with a wavelength of 1064nm for the altimetry measurements. To extend the mission life time, the operating period of the three lasers was non-permanent. The measurement campaigns lasted between 33 to 56 days, several times per year. The last operational period ended on 11$^{th}$ October 2009. Footprint size of the lasers is about 70m in diameter with a spacing of about 170m along record path. This varies with each laser period [14]. Hence the data distribution is point wise and no contiguous full coverage for the study site is available (Fig. 2). These ICESat GLAS data products are distributed by the National Snow and Ice Data Centre (NSIDC). There are 15 different standard data products, GLA01 to GLA15. The GLAS/ICESat L2 Global Land Surface Altimetry Data product GLA14 was used for this study. The most current two releases of NASA ICESat GLAS data products are Release-31 and Release-33. Because only Release-31 is available for all laser campaigns, it was used for this study [15]. The data is provided in scaled integer binary format and can be ordered through the ICESat/GLAS Data Subsetter provided by NSIDC [16]. Due to the reference to the TOPEX/Poseidon ellipsoid and EGM96 geoid, the coordinates need to be further processed.

The land use map applied by the Office for the Environment, Measurements and Nature Conservation of Baden-Württemberg (LUBW) contains 16 land use classes with a spatial resolution of 30mx30m [17]. Land use classes are: (1) urban dense, (2) urban sparsely, (3) industrial, (4) arable land, (5) wine/orchard, (6) mixed orchard, (7) fallow, (8) without vegetation, (9) intensive pasture, (10) extensive pasture, (11) coniferous, (12) deciduous, (13) mixed forest, (14) wind fall, (15) water, (16) wetland. The land use classification is based on Landsat images, captured during the year 2000.

Table 1 summarizes the elevation data sources, their specific geographic projection, the vertical reference system and the ground resolutions.

**Table 1** Summary of elevation sources

| Name | Projection | Ground Resolution |
|---|---|---|
| SRTM90 | WGS84/EGM96 | 90x90m |
| SRTM25 | WGS84/WGS84 | 25x25m |
| GDEMV2 | WGS84/EGM96 | 30x30m |
| ICESat\GLAS | TOPEX-Poseidon | point (x, y, z) |

## METHODOLOGY

The first step comprises a thorough pre-processing of ICESat data. Data from GLAS instrument is stored with unique record indexes where each record index contains 40 laser shots. Some data attributes are stored for the complete record index and others are recorded for each laser shot [18]. Variable names are indicated by unique flags of which the NSIDC provides an altimetry data dictionary with a detailed description

[18]. The GLAS land surface elevations are determined by several methods. The method used for each specific waveform is indicated by the 'i_ElvFlg' flag. According to this flag the elevation measurements used in this study have been calculated by the centroid of the received pulse between signal begin and signal end, defined for alternate parameterization (Fig.1). For further investigations we converted the ICESat GLA14 product from binary to ASCII format. NSIDC offers the tool 'IDL reader' to read data and print all the variables in ASCII format [19]. Since output data structure is not instantly suitable to transfer the records to a data base or preferred table format, order of ASCII data sets have been transposed and new columns with derived values were added. The necessary height transformation from TOPEX/Poseidon to WGS ellipsoidal heights was of importance for this study. A subtraction of geoid undulation values according to [20] was realised. In contrast to [20] we did not use a fixed height offset between TOPEX/Poseidon and WGS ellipsoids of 0.7m, but calculated the offset by the empirically derived formula provided by [21]. Geoid undulation is already given in GLA14 products; however it is only stored for the first and last shot for each record index. We calculated the undulation value for each shot, by linear interpolation between the first and last recorded value. Additional to the height transformation, we reduced the amount of records by filtering invalid or critical values by the following criteria:

a) Elevation use flag 'i_ElvuseFlg' indicating invalid elevations

b) Saturation correction flag 'i_satCorrFlg' indicating invalid correction value

c) Range offset quality flag 'i_rng_UQF' indicating invalid values

d) Cloud contamination flag 'i_FRir_qaFlag' indicating presence of clouds

e) Difference of GLAS height to high resolution DEM 'i_DEM_hires_elv' is more than 100m.

We stored all of the information provided in the GLA14 product in a database, but only latitude, longitude and the transformed height values were used for further evaluation in that study. A total of 14615 geolocations do comply with the requirements of data quality and existing elevation information of all DEMs inside the area under investigation.

The second step requires the transformation of datasets into a unique reference system. The elevation of the SRTM25 dataset refers to the WGS84 ellipsoid. As we want to calculate height differences based on EGM96, we transformed these values. The National Geospatial-Intelligence Agency (NGA) and NASA provide a WGS84 EGM96 15-Minute Geoid Height File and Coefficient File, as well a FORTAN program, named F77, to calculate undulation based on geographic coordinates [22]. For the centre coordinates of each SRTM25 pixel, the undulation was computed by the aforementioned software and finally subtracted from original values.

Height transformation was not necessary for the SRTM90 and GDEMV2 since they are already delivered in EGM96. Coordinate systems have been changed from geographic to map projection WGS 84 /UTM zone 32N. For the land use map a transformation from DHDN / Gauss-Krueger Zone 3 to UTM 32N WGS84 was computed within a Geographic Information System (GIS) using an equation based seven-parameter transformation.

In the third step, the ICESat footprint centre coordinates were used as template to extract elevation and land use information from the other data sources. We did not account for the footprint size or its shape. As well we did not spatially interpolate the raster values according to the location of the GLAS footprint centre inside each corresponding pixel. Finally the DEM values were subtracted from corresponding ICESat elevations.

At the time of this study there was no better possibility to get surface slope information, then to derive it from one of the available DEMs. We decided to take the newly released SRTM25, to calculate surface slope, being aware of the possible autocorrelation of results. Slope values have been grouped into different intervals. They are from 0° to 20° degrees in the range of one degree per interval, between 20° and 65° they are separated in 5° each interval.

## RESULTS

The 14615 sample locations, extracted at centre coordinates of ICESat footprints, are distributed within different land use classes. Within dense urban areas (1) 23 intersecting height values were observed, urban sparsely populated areas (2) 1085, (3) industrial areas 116, (4) arable land 3391, (5) wine/orchard 378, (6) mixed orchard 310, (7) fallow 18, (8) without vegetation 20, (9) intensive pasture 419, (10) extensive pasture 2911, (11) coniferous 1890, (12) deciduous 1765, (13) mixed forest 2057, (14) wind fall 143, (15) water 50 and wetland (16) 39.

Elevation differences for all locations, without any further data manipulation, have a mean value 0.4m with a RMSE 10.1 for SRTM90, -0.9m with RMSE 7.8 for SRTM25 and 0.8m with RMSE 9.3m for the GDEMV2 data set. Mean values and RMSE calculated with absolute values are 6.5m/7.8 for SRTM90, 5.2m/6.0 for SRTM25 and 6.9m/6.3 for GDEMV2. Figure 3 shows four different data plots. The median of each class is represented by the horizontal line inside each box. The dimension of each box indicates inner quartile range (IQR) of the first and third quartile. The upper and lower whiskers are calculated by multiplying the IQR by 1.5. This value is subtracted afterwards from the first quartile. The next higher value of the dataset determines lower whisker line. The upper whisker is calculated by starting from the third quartile. All data values, which exceed the whiskers, are plotted as dot. In figure 3 a-c, the height differences per land use class can be seen. High IRQs can be observed in the land use class coniferous forest (11), deciduous forest (12), mixed forest (13) and water (15). Lower IRQs and whisker ranges especially occur at land use type of arable land (4) and wine yards/ orchards (5). Figure 3c is of same plot type as the others and is illustrating the distribution of surface slope within the land use classes. Similar to plot 3a-b, land use classes 11, 12, 13 and 15 do have higher median values and higher whisker ranges. Due to small amount of samples inside the land use classes 1, 3, 7, 8, 15 and 16, the corresponding results should not further be considered.

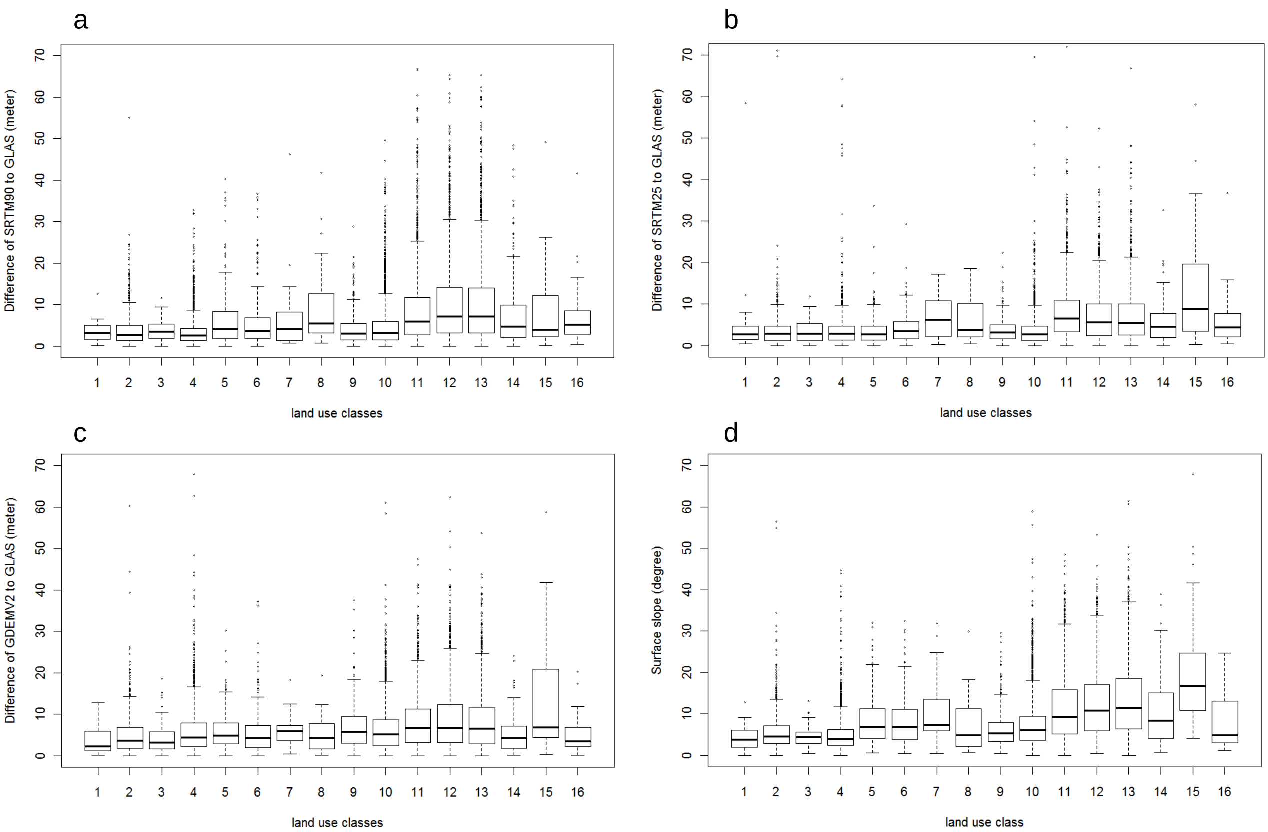


**Fig. 3 (a)** SRTM90 to GLAS elevation difference by land use **(b)** SRTM25 to GLAS elevation difference by land use **(c)** GDEMV2 to GLAS elevation difference by land use **(d)** Surface slope distribution inside land use classes. Land use classes: (1) urban dense, (2) urban sparsely, (3) industrial, (4) arable land, (5) wine/ orchard, (6) mixed orchard, (7) fallow, (8) without vegetation, (9) intensive pasture, (10) extensive pasture, (11) coniferous, (12) deciduous, (13) mixed forest, (14) wind fall, (15) water, (16) wetland

As described in the method section, a grouping of surface slope values into specified intervals was conducted. Fig.4, Fig.5 and Fig.6 illustrate the observed deviance between GLAS heights and DEM heights in relation to surface slope (absolute values in the range of 1° to 20°). Surface slope values are distributed inside the slope classes as follows: (1) 357, (2) 1026, (3) 1337, (4) 1521, (5) 1406, (6) 1227, (7) 1047, (8) 909, (9) 734, (10) 605, (11) 530,(12) 435 ,(13) 411,(14) 349, (15) 291, (16) 274, (17) 247, (18) 215, (19) 188, (20) 165, (25) 654, (30) 368, (35) 185, (40) 37, (45) 21, (50) 11, (55) 4, (60) 3, (65) 2 and 20 observations are above 65 degree. The distribution is right-skewed with a maximum of samples between 3° and 4° in class number 4 (Fig.7). The high difference between class 20 and 25 occurs because of a change in the interval range. The number of 1341 observations within all classes above 20° surface slope is relative small compared to the other 13274 observations, which are located between 0° and 20°. Linear regression of height differences and ungrouped original slope values in the range of zero to 20 degrees was conducted. With low $r^2$ values between 0.01 and 0.03 a significant relationship could not be found. Gradients for the linear function are 0.46/SRTM90, 0.25/SRTM25 and 0.13/GDEMV2.

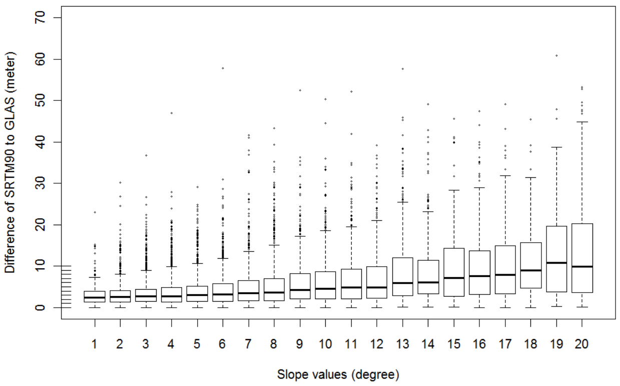


**Fig.4** Difference of SRTM90 to GLAS elevations by surface slope

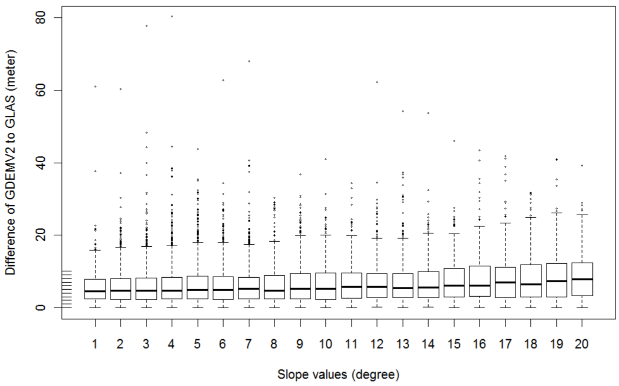


**Fig.5** Difference of GDEMV2 to GLAS elevations by surface slope

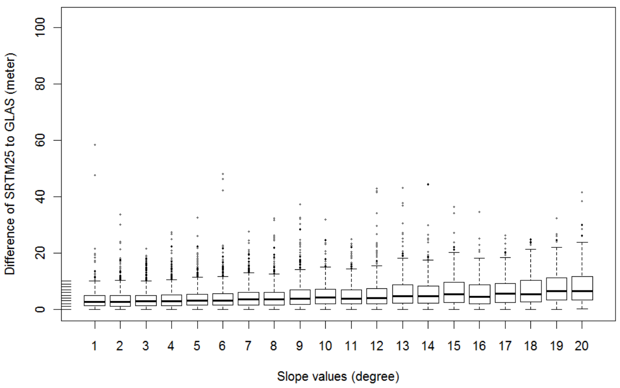


**Fig.6** Difference of SRTM25 to GLAS elevations by surface slope

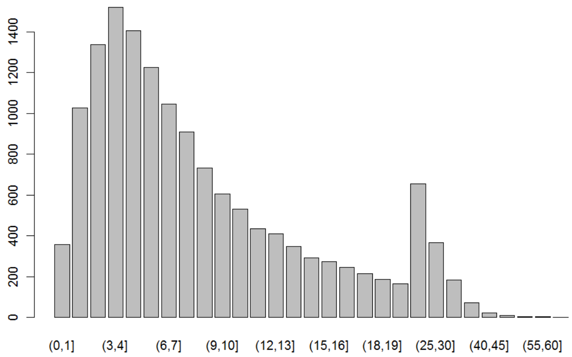


**Fig.7** Allocation of samples inside slope classes. Class value is upper range value (0°-1° = class 1)

## DISCUSSION AND CONCLUSION

Elevation differences have been analyzed under consideration of two potential influence factors: land use and surface slope. Related to land use classes we observed different values and mean variations of elevation differences. This implies that the land use class does affect elevation differences. Distribution of slope values inside the land use classes (Fig. 3d) is not the same in each class. Compared to other land use classes, the classes 11, 12, and 13 contain higher values of surface slopes. With regard to the forest types it is noticeable that these classes do have similar mean values. This statement can be observed for each DEM. The samples located in forested areas seem to be in more steep areas compared to the other land use classes (Fig. 3d). Two possibilities have to be further investigated. First, elevation measurements are different due to behaviour of different wavelengths (Fig.1) in relation to the type of land cover. Second, the strong influence of surface slope on height measurements covers any further influence by land use classes. The fact that we used SRTM25 data to calculate surface slope must be viewed critically, because it is well known that radar backscatter behaviour is strongly affected in mountainous areas. Further analyses should be carried out with an independent comparative data set from airborne LiDAR.

With regard to the method used for elevation extraction, we did not account the different resolutions of DEM sources. The extraction of raster values is based on the GLAS footprint centre location. It is not based on the footprint size and therefore not based on a spatial interpolation. For an accurate spatial interpolation, calculation of shape and energy distribution of each ICESat footprint should be done. This will be investigated in further studies with a combination of a high resolution DEM by airborne laser scanning.

Especially the method of GLAS elevation computation should be considered critically. In non-forested areas the method ‘centroid of signal end to signal begin’ for elevation computation may be sufficient. In forested areas the GLAS surface elevation does not represent the top of canopy or the bare ground (Fig. 1). For a more comparable study the behaviour of GLAS waveform on forested areas needs to be considered. A more adapted computation with respect to forest canopy by GLAS waveforms should make the GLAS elevations a better reference to evaluate the other elevation models in forested areas.

The results of this study are summarized below. Best elevation model for mountainous areas is the GDEMV2. It is least affected by rising surface slope. In flat areas, due to the higher ground resolution, the SRTM25 should be used. As well it has the lowest offset to ICESat data (5.2m), calculated by absolute differences. Further studies should adapt the ICESat elevation computation to the land cover.

## ACKNOWLEDGEMENTS

The authors are grateful to the ReCover consortium and the European Commission for supporting this research within the Seven Frame Work Programme FP7 (grand agreement no. 263075).

## REFERENCES

[1] Carabajal, C. C., Harding, D. J. (2005) ICESat validation of SRTM C-band digital elevation models. Geophys. Res. Lett 32 (22).

[2] Abshire, J. B., Sun, X., Riris, H., Sirota, J. M., McGarry, J.F., Palm, S., Yi, D., and Liiva, P. (2005) Geoscience Laser Altimeter System (GLAS) on the ICESat Mission: On-orbit measurement performance. Geophys. Res. Lett 32 (21).

[3] Braun, A., Fotopoulos, G. (2007) Assessment of SRTM, ICESat, and Survey Control Monument Elevations in Canada. Photogramm. Eng. Rem. Sens. 73 (12), S. 1333–1342.

[4] Rosette, J. A. B., North, P. R. J., Suarez, J. C., Los, S. O. (2010) Uncertainty within satellite LiDAR estimations of vegetation and topography. Int. J. Remote Sensing 31 (5), S. 1325–1342.

[5] Shtain Z., Filin S. (2011) Accuracy and reliability assessment of GLAS measurement over Israel. ISPRS Workshop, Laser scanning 2011, ISPRS, Volume XXXVIII, Calgary, Canada, conference proceedings.

[6] Huang, X., Xie, H., Liang, T., Yi, D. (2011) Estimating vertical error of SRTM and map-based DEMs using ICESat altimetry data in the eastern Tibetan Plateau. Int. J. Remote Sensing 32 (18), S. 5177–5196.

[7] Guosong Zhao, Huaiping Xue, Feng Ling (2010) Assessment of ASTER GDEM performance by comparing with SRTM and ICESat/GLAS data in Central China, 18th International Conference on Geoinformatics, pp.1-5, 18-20 June 2010

[8] Reuter, H.I., Nelson, A., Strobl, P., Mehl, W. Jarvis, A. (2009) A first assessment of Aster GDEM tiles for absolute accuracy, relative accuracy and terrain parameters. Geoscience and Remote Sensing Symposium, 2009 IEEE International, IGARSS 2009, vol.5, pp.V-240-V-243, 12-17 July 2009

[9] Carabajal, C. C. (2011), ASTER GLOBAL DEM VERSION 2.0 EVALUATION USING ICESat GEODETIC GROUND CONTROL, https://igskmncnwb001.cr.usgs.gov/aster/GDEM/GDEM_Validation_Documents.zip

[10] National Aeronautics and Space Administration NASA, http://icesat.gsfc.nasa.gov/icesat/science/measurements.php, 31.10.2011

[11] Farr, T.G., Rosen, P.A., Caro, E., Crippen, R., Duren, R., Hensley, S. et al. (2007): The Shuttle Radar Topography Mission. Rev. Geophys 45 (2).

[12] Deutsches Zentrum für Luft- und Raumfahrt, https://centaurus.caf.dlr.de:8443/eowebng/licenseAgreements/DLR_SRTM_Readme.pdf, 31.10.2011

[13] Tachikawa, T., Hato, M., Kaku, M. and Iwasaki A. (2011) The characteristics of ASTER GDEM version 2, IGARSS, July 2011.

[14] Zwally, H., (2004) Overview of the ICESat mission and results, Abstract #C21B-01, Proceedings of the American Geophysical Union Fall Meeting, December, San Francisco.

[15] Zwally, H.J., Schutz, R., Bentley, C., Bufton J., Herring, T., Minster, J., Spinhirne, J., Thomas, R. (2003) updated current year. GLAS/ICESat L2 Global Land Surface Altimetry Data V031, Acquired: February 2011 to March 2011. Boulder, CO: National Snow and Ice Data Center. Digital media 2011.

[16] National Snow and Ice Data Center (NSIDC) Distributed Active Archive Center (DAAC), ICESat/GLAS Data Subsetter, http://nsidc.org/data/icesat/order.html, 31.10.2011

[17] Landesanstalt für Umwelt, Messungen und Naturschutz Baden-Württemberg LUBW, http://www.lubw.baden-wuerttemberg.de, 31.10.2011

[18] National Snow and Ice Data Center NSIDC, http://nsidc.colorado.edu/data/docs/daac/glas_altimetry/data_dictionary.html, 31.20.2011

[19] National Snow and Ice Data Center NSIDC, http://nsidc.org/data/icesat/tools.html, 31.10.2011

[20] Bhang, K.J., Schwartz, F.W., Braun, A. (2007) Verification of the Vertical Error in C-Band SRTM DEM Using ICESat and Landsat-7, Otter Tail County, MN. IEEE Trans. Geosci. Remote Sensing 45 (1), S. 36–44.

[21] Haran, T. (2004) ftp://sidads.colorado.edu/pub/DATASETS/icesat/tools/idl/ellipsoid/README_ellipsoid.txt, 31.10.2011

[22] National Geospatial-Intelligence Agency NGA and NASA, http://earth-nfo.nga.mil/GandG/wgs84/gravitymod/egm96/egm96.html, 31.10.2011